Kissing-Loop Model of HIV-1 Genome Dimerization: HIV-1 RNAs Can Assume Alternative Dimeric Forms, and All Sequences Upstream or Downstream of Hairpin 248−271 Are Dispensable for Dimer Formation†

Michael Laughrea*,‡,§ and Louis Jetté‡

McGill AIDS Centre, Lady Davis Institute for Medical Research, Sir Mortimer B. Davis - Jewish General Hospital, and Department of Medicine, McGill University, Montréal, Québec, Canada

Received August 7, 1995; Revised Manuscript Received October 9, 1995⊗

ABSTRACT: The genome of all retroviruses consists of two identical RNAs noncovalently linked near their 5′ end. Dimerization of genomic RNA is thought to modulate several steps in the retroviral life cycle, such as recombination, translation, and encapsidation. The kissing-loop model of HIV-1 genome dimerization [Laughrea, M., & Jetté, L. (1994) *Biochemistry 33*, 13464−13474; Skripkin et al. (1994) *Proc. Natl. Acad. Sci. U.S.A. 91*, 4945−4949] posits that the 248−270 region of the HIV-1 genome, by forming a hairpin and initiating dimerization through a loop−loop interaction, is the full or at least the core dimerization domain of HIV-1 RNA. Here, we show by nested deletion analysis that the 3′ boundary of the HIV-1 dimerization domain is immediately downstream of hairpin 248−270 and that the isolated region 248−271 dimerizes at least as readily as longer RNAs. Among various HIV-1_{Lai} RNA transcripts containing hairpin 248−270, all form two types of dimer, as is implicit in the kissing-loop model. The high-stability dimer resists semidenaturing conditions and the low-stability dimer cannot, which is consistent with the model. At physiological temperatures, low-stability dimers are usually formed, as if dimerization without nucleocapsid proteins corresponded to loop−loop interaction without switching from intra- to interstrand hydrogen bonding. Our results show that the 3′ DLS (a sequence immediately 3′ from the 5′ splice junction and originally thought to be the dimerization domain of the HIV-1 genome) and adjacent nucleotides are not necessary for efficient dimerization of HIV-1_{Lai} RNA at low and high ionic strength. Upstream of hairpin 248−270 exists another "DLS-like" sequence that we name 5′ DLS: like the isolated 3′ DLS, the isolated 5′ DLS forms an apparently nonphysiological structure that can become substantially dimeric at high ionic strength.

Retroviruses are a family of RNA viruses that replicate through a DNA intermediate, and human immunodeficiency virus type 1 (HIV-1)[1] is a retrovirus acknowledged as a cause of the acquired immunodeficiency syndrome (AIDS). The genome of all retroviruses, including HIV-1, is formed of two identical RNAs that are non-covalently linked near their 5′ ends (Marquet et al., 1994, and references therein). Dimerization of this diploid genome might modulate several steps of the retroviral life cycle, such as (i) translation of the genome into viral proteins; (ii) preferential packaging (or encapsidation) of two genomic RNAs within the budding viral shell (or capsid) against a vast excess of cellular RNAs; (iii) recombination between the two homologous genomic RNAs in order to increase the rate of viral evolution and to bypass occasional breaks in one of the genomic RNAs; (iv) stabilization of the genome against degradation; (v) reverse transcription (Laughrea & Jetté, 1994, and references therein). Dimerization of genomic RNA could constitute a suitable anti-AIDS therapeutic target, but little is known about the mechanism of retroviral genome dimerization.

The primer binding site and the 5′ splice junction of HIV-1 RNA are separated by 90 nucleotides (nts) extending from U200 to G289 in HIV-1_{Lai}. This region represents two-thirds of the leader sequence (the other third goes from the 5′ splice junction to AUG338, the initiation codon of the *gag* gene). It contains an encapsidation (Kim et al., 1994) and an in vitro dimerization signal (Laughrea & Jetté, 1994; Skripkin et al., 1994). Both signals strongly overlap; at current level of resolution, they could be identical, or more precisely, the dimerization signal could be a subset of a larger encapsidation signal (Méric & Goff, 1989; Levin et al., 1974). Since HIV-1 genome dimerization might precede or be required for proper encapsidation (Fu et al., 1994; Méric & Goff, 1989; Levin et al., 1974), it seems useful to investigate the nature of the in vitro HIV-1 dimerization signal, the mechanism of in vitro genome dimerization, and the properties of dimeric HIV-1 RNA transcripts.

The properties of the dimerization signal identified by us (Laughrea & Jetté, 1994) and Skripkin et al. (1994) have led us and them to propose what we call the kissing-loop model of HIV-1 genome dimerization. According to this

† This work was supported by a grant from the Medical Research Council of Canada to M.L.

* To whom correspondence should be addressed at the Lady Davis Institute for Medical Research, 3755 Côte Ste. Catherine Road, Montreal, Quebec, Canada H3T 1E2. Tel: (514) 340-8260. Fax: (514) 340-7502.

‡ Lady Davis Institute for Medical Research.

§ McGill University.

⊗ Abstract published in *Advance ACS Abstracts,* January 15, 1996.

[1] Abbreviations: HIV-1, human immunodeficiency virus type 1; AIDS, acquired immunodeficiency syndrome; nt, nucleotide; bp, base pair; 3′ DLS, name of a sequence starting very near the 5′ splice junction (typically at nt 295) and ending at nt 401; TBM/RT, buffer TBM and at room temperature; TBE_2/27 °C, buffer TBE_2 and in a room maintained at 27 °C; 5′ DLS, name of an RNA sequence ending in or near the U5 region and which can dimerize in high-salt conditions; SEM, standard error of the mean.

0006-2960/96/0435-1589$12.00/0

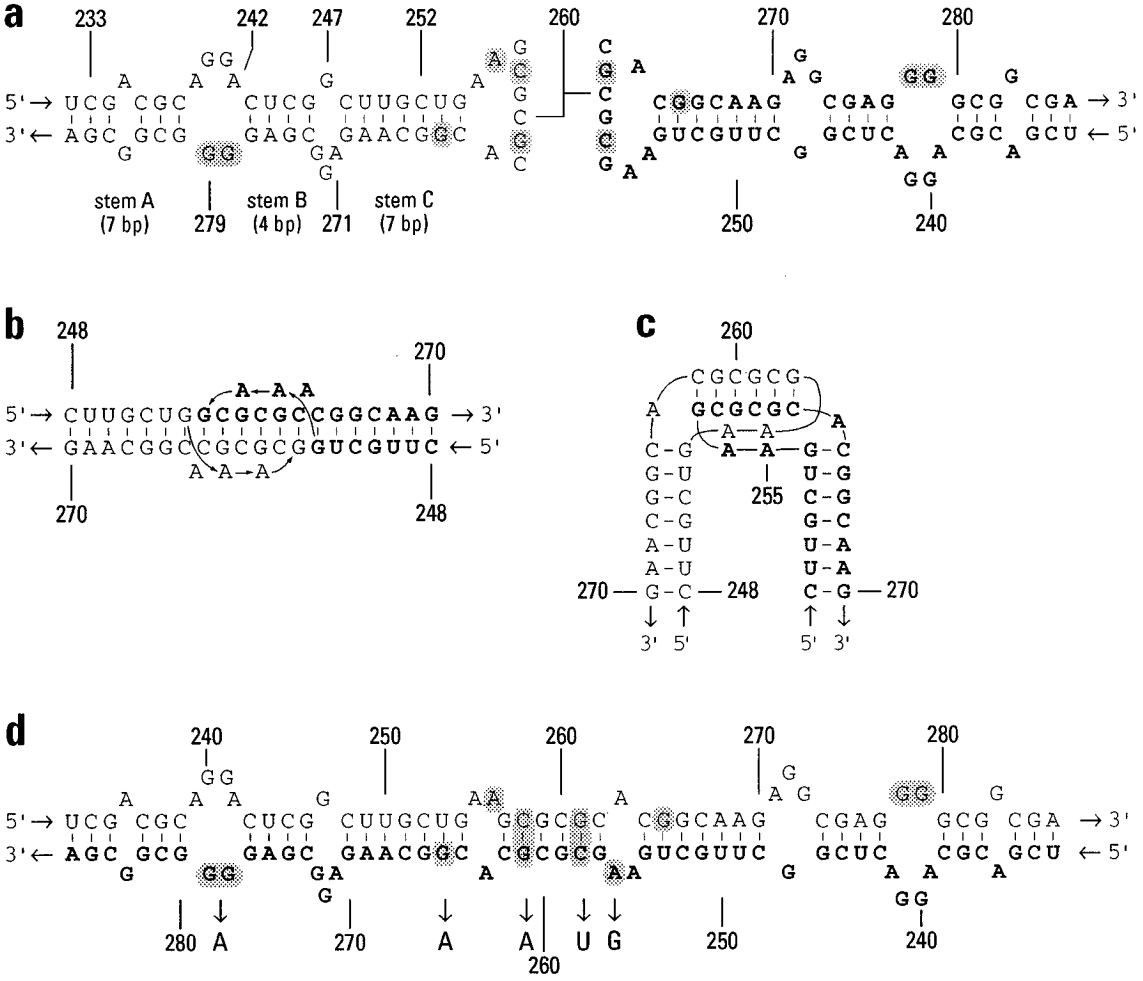

FIGURE 1: Secondary and tertiary structure model for the 232−286 region of HIV-1 RNA as (a) a monomer, (b and c) a loose dimer, and (d) a tight dimer. In a and d, nucleotides that differ in HIV-1_{Mal} and HIV-1_{LaipB2} are shadowed, and the corresponding HIV-1_{Mal} nucleotides are indicated by arrows in the bottom part of d. (a) Postulated stem−loop structure of two monomers with their respective GCGCGC262 almost ready to hydrogen-bond to each other [from Laughrea and Jetté (1994)]. (b,c) Possible secondary structures of the loose dimer. (d) Possible secondary structure of the tight dimer with one strand in bold characters and the other in normal characters. Loose and tight dimers are defined in the Results.

model (i) the primary dimerization site is a 6-nt long autocomplementary sequence located at nucleotides 257−262 of the HIV-1_{Lai} genome (274−279 in HIV-1_{Mal}; for simplicity, all further positions will be converted into HIV-1_{Lai} positions, whether or not the work was done with HIV-1_{Lai}), (ii) the autocomplementary sequence is at the apex of a hairpin loop formed by nucleotides 248−270 or 233−285,[2] (iii) two autocomplementary sequences bind to each other, forming first a 6-base-pair (bp) Watson−Crick duplex (Figure 1a,b) and perhaps later a 20−40-bp complex (Figure 1d), and (iv) hairpin 248−270 or hairpin 233−285 is the full or at least the core dimerization domain of the HIV-1 genome. A dimerization domain is the shortest dimeric sequence that mimics the dimerization properties of protein-free HIV-1 genomes. A core dimerization domain is a subset of the dimerization domain, i.e., a smaller dimer whose relevant physicochemical properties (e.g., kinetics of dimerization, stability of the dimer) fall short of matching those of longer sequences or of HIV-1 genomic RNA (Laughrea & Jetté, 1994). The idea that the 233−285 region forms a hairpin with a 6-nt autocomplementary sequence in the middle of a 9-nt loop is consistent with our own footprinting studies (Laughrea & Jetté, 1994) and those of Harrison and Lever (1992) and Baudin et al. (1993).

The kissing-loop model had been tested in two ways at the inception of this project. It was known that the integrity of the autocomplementary sequence and of the 5′ strand of stem C (Figure 1a) is essential for dimerization: (i) RNAs with the first 3 nts of the autocomplementary sequence replaced by AAA cannot dimerize (Skripkin et al., 1994); (ii) RNAs starting at C252 cannot dimerize, while RNAs starting at C248 dimerize very well, and RNAs starting at U249 dimerize to a much smaller extent (Laughrea & Jetté, 1994). It was also known that regions 242−342 (Laughrea & Jetté, 1994) and 1−295 (Marquet et al., 1994) are sufficient to respectively obtain excellent and significant dimerization yields, suggesting that a core dimerization domain of HIV-1_{Lai} RNA is located within the 242−295 region. It is noteworthy that deletion of the 241−253 region of the HIV-1_{Lai} genome reduces by 80%−85% the amount of intact genomic RNA per virion recovered from MT4 cells (Kim et al., 1994). The dimerization signal under study is therefore also an encapsidation signal, i.e., a region

[2] Out of 21 sequenced HIV-1 leader sequences, 21 can form a 248−270 hairpin but only 20 can form a 233−285 hairpin as drawn in Figure 1 because of one C→A281 transversion (Myers et al., 1993). Thus the 248−270 hairpin is more universal than the 233−285 hairpin but the 233−285 hairpin remains highly phylogenetically conserved.

of high physiological significance.

The purpose of this paper is to test three more predictions of the kissing-loop model of HIV-1 RNA dimerization. (i) Sequences smaller than the 242−295 region (and at least as large as the 248−270 region) should be *sufficient* to obtain excellent dimerization yields. (ii) RNAs containing region 248−270 or 233−285 should form two types of dimers (one presumably less stable than the other) no matter the location of the 5′ or 3′ end. This is of immediate physiological interest since immature virions contain a dimeric HIV-1 genome that is less stable than in mature virions (Fu et al., 1994). We emphasize that our goal is *not* to test whether the dimeric structures displayed in Figure 1b,d (co)exist, but simply to test whether *two* types of dimers can be formed from HIV-1 RNAs and to delimit their 5′ and 3′ boundaries. Figure 1b−d merely illustrates what these two types of dimers might look like. (iii) The 3′ strand of stem C should be essential for obtaining any dimerization or for obtaining two types of dimers. This paper will show that the kissing-loop model of HIV-1 genome dimerization successfully meets the three tests. We will also show that the 3′ DLS (a sequence immediately downstream from the 5′ splice junction and originally thought to be the dimerization domain of the HIV-1 genome) and adjacent nucleotides are not necessary for efficient dimerization of HIV-1_{Lai} RNA at low and high ionic strength.

EXPERIMENTAL PROCEDURES

Buffers. Buffer L (Marquet et al., 1991; Laughrea & Jetté, 1994): 50 mM sodium cacodylate (pH 7.5), 40 mM KCl, and 0.1 mM $MgC1_2$. Buffer H (Marquet et al., 1991; Laughrea & Jetté, 1994): 50 mM sodium cacodylate (pH 7.5), 300 mM KCl, and 5 mM $MgC1_2$. TBM (Laughrea & Moore, 1977; Laughrea & Jetté, 1994; Marquet et al., 1994): 89 mM Tris, 89 mM borate, and 0.1 mM $MgCl_2$. $TBE_{0.5}$, TBE_1, TBE_2, and TBE_3 (Peacock & Dingman, 1967): as TBM but with the $MgCl_2$ replaced by 0.5, 1, 2, or 3 mM EDTA, respectively.

Materials. Restriction enzymes *Dra*I, *Hin*dIII, *Acc*I, *Hae*III, *Rsa*I, *Hha*I, *Taq*I, *Mae*III, and *Bgl*II were from Pharmacia (Montreal, Quebec). Restriction enzymes *Bso*fI, *Eco*57I, *Hga*I, and *Hin*P1I were from New England Biolabs (Mississauga, Ontario). Restriction enzymes *Mae*I, *Bss*HII, and *Tru*9I were from Boehringer Mannheim (Montreal, Quebec). Agarose, electrophoresis grade, was from ICN.

Plasmid Construction. All plasmids described in this paper have a fraction of the HIV-1_{Lai} genome cloned immediately (or a few nucleotides) downstream from a strong T7 RNA polymerase promoter. pLJ plasmids have also an SP6 RNA polymerase promoter at the other end of the multiple-cloning site, permitting synthesis of antisense HIV-1 RNA transcripts. Plasmids pBL, pB233, pLJ230, pLJ232, pLJ242, pLJ246, pLJ248, pLJ249, and pLJ252 have been described in Laughrea and Jetté (1994). They yield T7 transcripts respectively starting at nucleotide 1, 233, 230, 232, 242, 248, 249, and 252 of the HIV-1 genome. pLJ230′ is pLJ230 cut with *Hin*dIII and religated.

RNA Synthesis and Recovery. Prior to T7 RNA polymerase transcription, plasmids pB233, pBL, and pLJ were cleaved with *Hae*III (G401 of HIV-1_{Lai} RNA), *Acc*I (G508), *Hin*dIII (U635), or *Dra*I (U790), respectively. The end result was various control RNAs all containing the dimerization domain. In experiments designed to define the 3′ boundary of the dimerization domain, the same plasmids were variously cleaved with *Mae*I, *Rsa*I, *Bso*fI, *Eco*57I, *Mnl*I, *Bss*HII, *Hha*I, *Hga*I, *Taq*I, *Hin*P1I, *Mae*III, or *Tru*9I to obtain a collection of RNAs ending at nucleotide 314, 295, 282, 271, 262, 261, 257/259, 248, 234, 186, 125, and 66, respectively. In one experiment, plasmid pLJ230′ was cut with *Bgl*II and transcribed by SP6 RNA polymerase: this produced antisense RNA 636−232, a 420-nt RNA that is the antisense of the 232−636 region of the HIV-1 genome (and that has pppGAACUCGAGCAGCUG, i.e., 15 additional nucleotides derived from the polylinker, 5′ to the antisense of U636). Transcription and RNA recovery was done using the MEGAscript kit of Ambion (Austin, Texas). In short, after transcription had proceeded for 6 h, DNase I was added, followed 15 min later by addition of ammonium acetate stop solution and extraction with phenol/chloroform.

In Vitro Dimerization of HIV-1 RNA Transcripts (Laughrea & Jetté, 1994). A 500-ng to 3-μg amount of RNA dissolved in 8 μL of water was heated for 2 min at 92 °C and chilled for 2 min on ice. 2 μL of 5× concentrated buffer L or H was added, and (unless otherwise stated) the samples were incubated for 30 min at 0 °C in buffer L (low-salt conditions) or at 37 °C in buffer H (high-salt conditions). The samples were loaded on 3% agarose gels after addition of 2 μL of loading buffer containing glycerol. Electrophoreses were run at 4−5 W at room temperature, 4, 27, and 37 °C as indicated, using the GNA-100 submarine gel electrophoresis unit of Pharmacia. The electrophoresis (and gel) buffers were TBM, $TBE_{0.5}$, TBE_1, TBE_2, or TBE_3 as indicated. Electrophoresis lasted 70−100 min, i.e., long enough to accumulate 6000−7000 V·min. After electrophoresis the gels were stained in 2 μg of ethidium bromide/mL for 10 min, and the percentage of dimerization was estimated by visual inspection or by scanning the photographic negatives with an LKB Ultroscan XL laser densitometer. Denatured samples were prepared by incubation at room temperature for 10 min in the presence of 64% formamide and 0.45% formaldehyde (Laughrea & Jetté, 1994).

RESULTS

The 3′ Boundary of the Dimerization Domain: Nested Deletion Analysis. Plasmids pBL, pB233, pLJ242, and pLJ248 were linearized at G508 or at various positions upstream of G315 prior to transcription. Our goal was to define the 3′ boundary of the dimerization domain of the HIV-1 genome. Nineteen RNAs were produced. They started at G1, C233, A242, or C248 of the HIV-1 genome and ended at A66, C125, G186, G234, C248, G261, C262, A271, G282, U295, A314, or G508. They were incubated in low-salt conditions (low temperature and low ionic strength) and electrophoresed at room temperature in a 3% agarose gel containing buffer TBM (Figure 2). The numbers in the name of an RNA refer to its first and last HIV-1 RNA nucleotide. Low-salt conditions were adopted because they yield HIV-1_{Lai} RNAs that are 50%−100% dimeric, while leaving completely monomeric HIV-1 RNAs lacking the 1−251 or the 233−251 region (Laughrea & Jetté, 1994). Electrophoresis in TBM at room temperature (TBM/RT) was adopted because the dimericity of each RNA studied by Laughrea and Jetté (1994) was the same in TBM/RT and in TBM/4 °C (not shown).

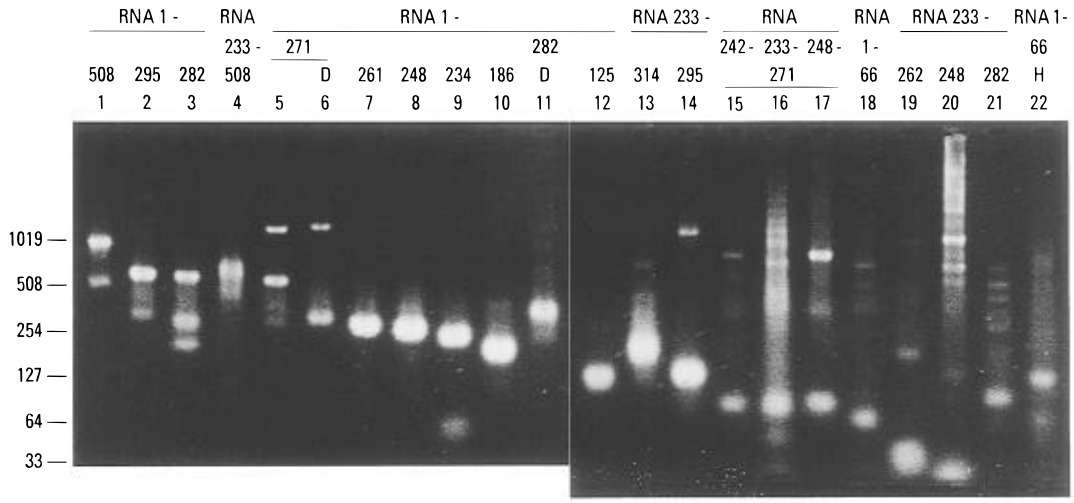

FIGURE 2: In vitro dimerization of 19 RNAs containing part or all of the first 508 nts of HIV-1 genomic RNA. Each successive lane usually displays a shorter RNA. A list of the RNA monomeric lengths follows. Lane 1, 509 nt; lane 2, 296; lanes 3 and 11, 283; lane 4, 279; lanes 5 and 6, 272; lane 7, 262; lane 8, 249; lane 9, 235; lane 10, 187; lane 12, 126; lane 13, 85; lane 14, 66; lane 15, 46; lane 16, 42; lane 17, 39; lanes 18 and 22, 67; lane 19, 33; lane 20, 19; lane 21, 53. Far left: a size scale, expressed in number of nt. All RNAs were incubated in low-salt conditions except for lanes 6 and 11, which display denatured (D) RNAs, and lane 22, which displays an RNA incubated in high-salt (H) conditions. Three percent agarose gel electrophoresis (100 V, 70 min) was in TBM at room temperature. The temperature of the electrophoretic buffer was 28 °C, i.e., 6 °C higher than room temperature. The low-mobility band or smear present in lanes 5 and 6 and 13−22 represents RNAs of unknown sequence that for a variety of reasons (e.g., incomplete plasmid cleavage coupled to poor transcription yield of short templates) can be produced during a transcription reaction. RNA 1−282 had two monomer bands.

Figure 2 shows the electrophoretic mobility of these RNAs. RNAs 1−271 and 1−282 (lanes 6 and 11) are in addition displayed in the denatured state to help the reader assess the dimeric or monomeric character of each displayed RNA. The 19 RNAs of Figure 2 *form two neat classes*. (i) The 11 RNAs ending *downstream of G270* were completely or significantly dimeric (lanes 1−5 and 13−17). (ii) The eight RNAs ending *upstream of A263* were completely monomeric (lanes 7−10 and 18−20). These results indicate that the 3′ boundary of the dimerization domain is located *somewhere between A263 and A271* (compare lane 16 to lane 19, or lane 5 to lane 7) and that the 248−271 region is *sufficient* for HIV-1 RNA dimerization (compare lane 17 to lane 18). There was no improvement in dimer yield as the 3′ end was moved downstream from A271 (compare lane 1 to lane 5). It was previously thought that the dimerization domain of the HIV-1 genome was located in the 295−401 region (Laughrea & Jetté, 1994, and references therein). The 295−401 region is called the 3′ DLS (see below). Figure 2 clearly shows that the 3′ DLS is not necessary for efficient dimerization of HIV-1 RNA (compare lane 2 to lane 1, and lane 14 to lane 4).

In control experiments (mostly not shown), the electrophoretic mobility of each RNA of Figure 2 was examined after denaturation (which made all of them 100% monomeric) and after incubation in high-salt conditions (which made 100% dimeric or nearly so those RNAs, such as 1−508, 1−295, and 1−282, that were 30%−75% dimeric in low-salt conditions). More specifically, after denaturation, all RNAs that seemed dimeric moved as if size had been cut 50% or 40%−45% in some cases, and all RNAs that seemed monomeric were unchanged in mobility or appeared 10%−20% larger in some cases (one cannot expect denatured RNAs to have exactly the mobility of a monomer or a half-dimer because some denatured RNAs may have a more open, i.e., slower, structure than native monomers). When log [no. nt] of each dimer and monomer was plotted as a function of electrophoretic mobility, a straight line was formed from

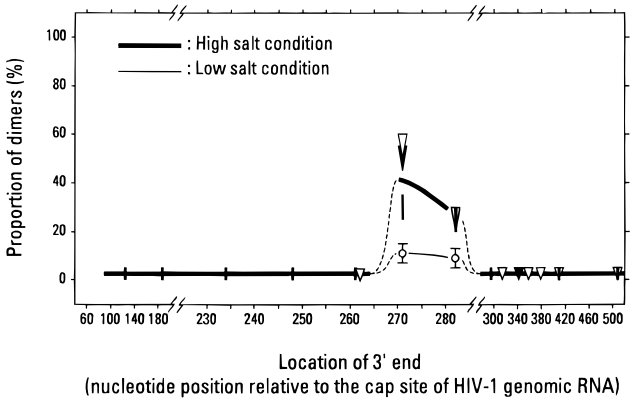

FIGURE 3: Dimerization in high-salt (thick line) or low-salt (thin line) conditions, as assayed by electrophoresis in TBE_2/27 °C. Error bars denote SEM. Where not visible, the thin line overlaps the thick one. Vertical bars, RNAs 1−...; ▽, RNAs 233−...; ▼, RNAs 242−... The height of each symbol reflects the range of results obtained. Electrophoretic conditions: 70 V, 100 min.

1018 to 33 nt (not shown). RNAs that were ≤33-nt long moved more slowly than expected because they were close to the limit of resolution of 3% agarose.

One HIV-1 RNA—Two Dimeric Forms. Comparative Electrophoresis Reveals Two Kinds of Dimeric RNAs. The kissing-loop model predicts two dimeric forms for the dimerization domain. They have been presented in the introduction (compare Figure 1b to d). The distinct conformations in Figure 1b,d might differentially resist to electrophoresis in native and semi-denaturing conditions. Accordingly, our RNAs were electrophoresed in buffers and ambient temperatures ranging from TBM in the cold room (TBM/4 °C) to TBE_3 in the 37 °C room (TBE_3/37 °C). We settled on TBM/RT and TBE_2/27 °C. Room temperature is 21−22 °C.

The RNAs of Figure 2 were next electrophoresed in TBE_2/27 °C. The results are shown in Figure 3. RNAs ending *upstream of A263* were monomers, as in Figure 2. In

contrast to Figure 2, RNAs ending *downstream of G270* divided themselves into two categories. (i) *All RNAs ending downstream of G294 were completely monomeric, contrary to their behavior in TBM/RT* (compare the right-hand side of Figure 3 to lanes 1 and 2 of Figure 2, lane 1 of Figure 2 to lane 1 of Figure 5, and lane 3 of Figure 8 to lane 9 of Figure 8). (ii) All RNAs ending at A271 or G282 were somewhat dimeric, but much less so than in Figure 2 (compare middle of Figure 3 to lanes 3, 5, 16 and 21 of Figure 2). Incubating the RNAs of Figure 3 in high-salt conditions (37 °C and high ionic strength) prior to electrophoresis changed nothing to the status of the monomeric RNAs (for example, see lanes 1 and 7 of Figure 6), but the partly dimeric RNAs became more dimeric (thick line of Figure 3; lanes 4 and 11 of Figure 6). The significant result is that RNAs ending downstream of G294 are low-stability dimers. We shall call them loose dimers. Loose dimers are defined as RNAs that are fully or partially dimeric after electrophoresis in TBM/RT but completely monomeric after electrophoresis in TBE_2/27 °C.[3] Tight dimers are defined as RNAs that are *as dimeric* in TBE_2/27 °C as they are in TBM/RT. RNAs ending at A271 or G282 were three to eight times more dimeric in TBM/RT than in TBE_2/27 °C. They seem to be a mixture of loose and tight dimers rather than dimers of intermediate stability, for two reasons. (i) The proportion of dimers among RNAs ending at A271 and G282 was 150%−200% higher in high-salt conditions than in low-salt conditions when assayed by electrophoresis in TBE_2/27 °C (Figure 3); it was only 50% higher when comparison was done after electrophoresis in TBM/RT (see below). (ii) There is no evidence that dimers of RNAs ending at A271 or G282 dissociate over the whole duration of the electrophoresis in TBE_2/27 °C instead of breaking down within 15 min as loose dimers do: Figures 5 and 6 will show that the smears between monomer and dimer bands were similar to the smears associated with loose dimer dissociation during electrophoresis in TBE_2/27 °C.

After incubation in buffer L for 30 min at 37 °C and electrophoresis in TBE_2/27 °C, all RNAs ending at A271 and G282 were as dimeric as in high-salt conditions (compare lanes 4 and 11 of Figure 5 to lanes 4 and 11 of Figure 6), suggesting that formation of tight dimers in high-salt conditions is promoted by increased temperature rather than by increased salt concentration. Will RNAs ending downstream of G294 become tight dimers after incubation at >37 °C?

All Deletion-Free RNAs Ending Downstream of G270 Can Form Two Kinds of Dimers. Figure 4 mimics Figure 3 except that each RNA was incubated at 60 °C for 10 min before electrophoresis. RNAs ending upstream of A263 again remained monomeric (as in Figure 2). But the second half of Figure 4 looks like lanes 1 and 2 of Figure 2 rather than of Figure 3, indicating that the heat treatment had substantially transformed all RNAs ending downstream of G294 into tight dimers (compare lanes 1 and 7 to lanes 2 and 9 of Figure 5). Moreover, RNAs ending at A271 and

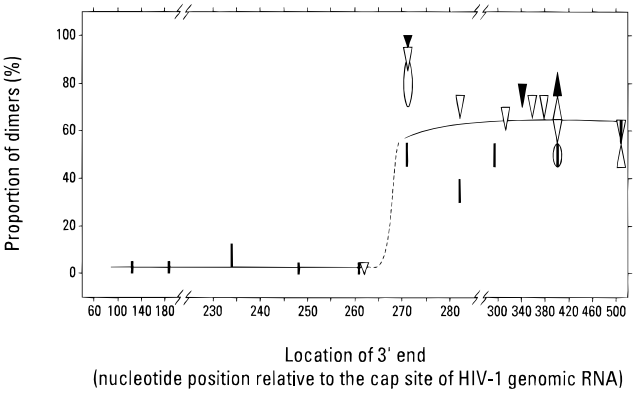

FIGURE 4: Dimerization of HIV-1 RNAs after a 60 °C heat treatment and electrophoresis in semi-denaturing conditions. As in Figure 3 except that incubation was in low-salt conditions followed by a 10-min postincubation at 60 °C. Oval-shaped symbol, RNAs 248−...; △, RNAs 230−...; ▲, RNA 232−401; the other symbols have been defined in Figure 3.

G282 have become on average more dimeric than in Figure 3 (compare lanes 11, 15, and 19 to lanes 12, 17, and 20 of Figure 6). It follows from Figures 2−4 that one and the same HIV-1 RNA, as long as it ends downstream of A270, can assume alternative dimeric forms depending on the incubation protocol. Two gel electrophoretic proofs of these alternative dimeric forms are shown by comparing lane 1 of Figure 2 to lanes 1 and 2 of Figure 5 and by comparing lane 3 of Figure 8 to lanes 8 and 9 of Figure 8. It is seen that RNAs 1−508 and 233−635 can appear mostly dimeric (lane 1 of Figure 2; lane 3 of Figure 8) or completely monomeric (lane 1 of Figure 5; lane 9 of Figure 8) depending on whether the electrophoresis is in TBM/RT or TBE_2/27 °C. This represents evidence for the loose dimer form of RNAs 1−508 and 233−635. Lane 2 of Figure 5 and lane 8 of Figure 8 show that a new type of dimer (the tight dimer form) appears when RNAs 1−508 and 233−635 are heated at 60 °C prior to electrophoresis in TBE_2/27 °C. Other proofs involve RNA 233−282 (compare lane 21 of Figure 2 to lanes 15 and 16 of Figure 5), RNA 1−295 (compare lane 2 of Figure 2 to lanes 4 and 6 of bottom panel of Figure 5), and RNA 233−508 (compare lane 4 of Figure 2 to lanes 7 and 9 of Figure 5).

55−65 °C Is Optimal for Formation of Tight Dimers by RNAs Ending Downstream of G294. The effect of incubation temperature on the formation of tight dimers by various HIV-1 RNAs is presented in Figure 5 (incubations in low salt) and in Figure 6 (incubations in high salt). These figures serve also as electrophoretic documentation for some data points of Figures 3 and 4. In low-salt conditions plus 10 min at 50 °C, RNAs 1−401 and 1−508 were as dimeric as RNA 1−508 in high-salt conditions plus 10 min at 70 °C; in high-salt conditions plus 10 min at 50 °C, they were <10% dimeric (not shown). Additional experiments at 50, 55, 60, 65, and 70 °C done with these and other RNAs (such as 1−790, 233−790, 248−790, etc.) showed that the optimal temperatures for formation of tight dimers in buffers L and H were respectively 55−60 and 65 °C for RNAs ending 3′ of G282 (not shown). Lanes 4−6 and 11−22 at the top of Figures 5 and 6 show that a considerable proportion of RNAs 1−282 and 1−271 are tight dimers at 37 °C. A 10-min incubation at 50 °C more than doubled the dimer yield of RNAs 233−271 and 242−271 (lane 20 of Figures 5 and 6), and RNA 233−282 achieved its highest proportion of dimers

[3] With RNAs containing the 248−294 region and incubated in high-salt conditions, the yield of loose dimers went progressively down according to the electrophoretic sequence TBM/RT = TBM/4 °C = TBE_2/4 °C > TBE_2/RT ≥ TBE_2/27 °C = TBE_2/37 °C. In TBE_2/RT, the percentage of dimer was 20% on average and variable (from 0% to 50% depending on the RNAs and/or the experiment), while in TBE_2/27 °C it was always <5% for each RNA and in each experiment.

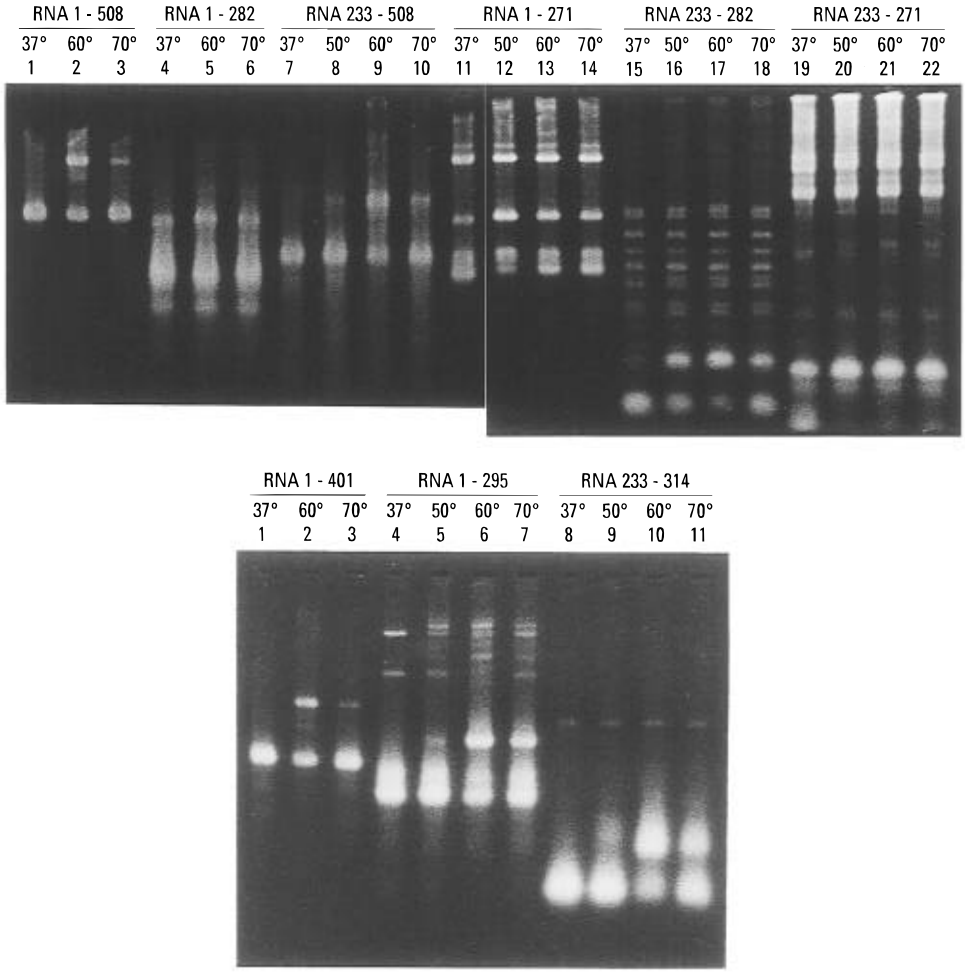

FIGURE 5: Dimerization of RNAs 1−508, 1−401, 1−295, 1−282, and 1−271 and 233−508, 233 −314, 233−282, and 233−271 as assayed in TBE_2/27 °C. RNAs were incubated and electrophoresed as in Figure 3 except that preincubation in low-salt conditions was followed by a 10-min incubation at the indicated temperatures prior to electrophoresis. In lanes 11−22 of the top panel and 4−11 of the bottom panel, high molecular weight bands or smears do not correspond to the RNAs of interest.

at 60 °C (lane 17 of Figures 5 and 6). Under identical conditions RNA 248−271 was more than 80% dimeric (not shown).

Elementary Kinetics of Tight Dimerization. Yields of tight dimers were not improved by incubating each RNA of Figure 5 for 20, 40, and 60 min in buffers L and H at their optimal formation temperature, or, for RNAs that had never formed tight dimers, at 50, 60, and 70 °C (not shown). In fact, half-maximal yields were typically reached in 40 s to 1 min at 60 °C in buffer L (M. Laughrea and L. Jetté, submitted). With RNAs variously ending at nucleotide 295, 314, 359, 378, 401, 508, 635, or 790, incubations at 45 °C in buffers L or H typically yielded ≤5% tight dimers after 1 h and 10%−20% tight dimers after 5 h (not shown). We conclude that the rate of formation of tight dimers is 2−3 orders of magnitudes slower at 45 °C than at 60 °C.

We have also observed that RNAs 252−401, 252−508, and 1−401Δ233−251, which cannot dimerize even after 3-h incubations in high-salt conditions (Laughrea & Jetté, 1994; data not shown) could not dimerize at 50, 60, or 70 °C in buffers L or H, and that RNAs 249−401 and 249−790, which dimerize much less than RNAs 248−401 and 248−790 at ≤37 °C (Laughrea & Jetté, 1994, and data not shown) formed 50%−60% fewer tight dimers than RNAs 248−401 and 248−790 at 60 °C (not shown). These data, together with previous ones (Laughrea & Jetté, 1994), suggest that a short stem C inhibits formation of both loose and tight dimers. As far as we have tested, any HIV-1 RNA that can form a tight dimer can form a loose dimer and any HIV-1 RNA that can form a loose dimer in low-salt conditions can form a tight dimer. Tight and loose dimers that contain region 248−270 appear to have identical 5′ and 3′ boundaries.

Nested Deletions Analyzed in High-Salt Conditions. We had shown that after incubation in high or low-salt conditions and electrophoresis in TBM/4 °C HIV-1 RNAs lacking the 1−251, the 233−251, or larger regions were completely monomeric while more complete HIV-1 RNAs were more dimeric in high-salt than in low-salt conditions (Laughrea & Jetté, 1994). In at least these instances, high-salt conditions were thus preferable to low-salt conditions for differentiating between RNAs possessing and lacking the full 248−270 region. However, consistent with simple theory according to which high ionic strength can promote additional, possibly artefactual interactions between RNA molecules (Bloomfield et al., 1974), Figure 7 shows that high-salt conditions do not always magnify differentiations seen in low-salt conditions: RNAs 1−66, 1−125, and 1−186, though appearing monomeric in low-salt conditions, no matter the electrophoresis protocol (Figures 2 and 3), or after electrophoresis in TBE_2/27 °C, no matter the incubation protocol (Figures 3 and 4), were >60% dimeric after

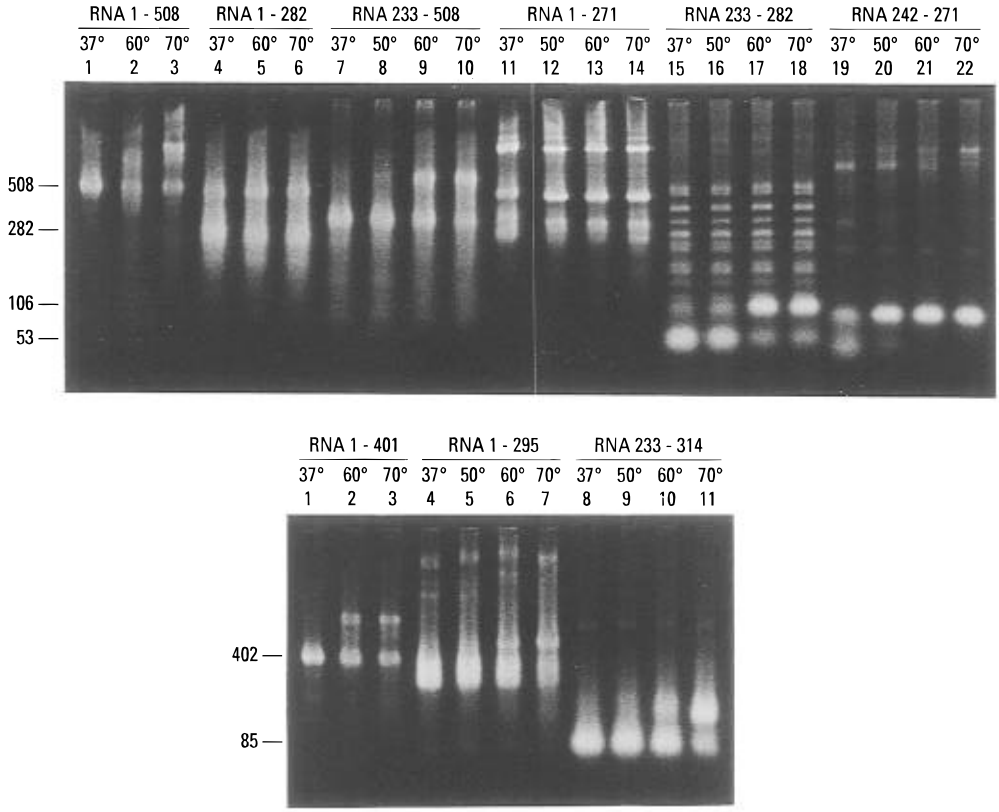

FIGURE 6: Dimerization in high-salt conditions, as assayed by electrophoresis in TBE_2/27 °C. As in Figure 5, except that preincubation was in high-salt conditions and that RNA 233−271 was replaced by RNA 242−271.

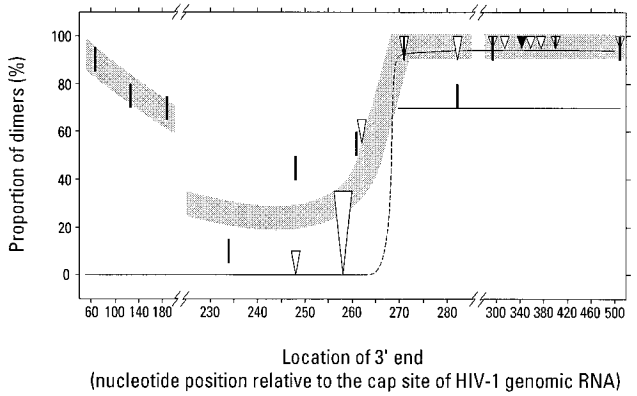

FIGURE 7: Dimerization of HIV-1 RNAs at high ionic strength, as assayed by electrophoresis in TBM/RT. As in Figure 2 except that the RNAs were incubated in high-salt conditions prior to electrophoresis. RNAs 248−271 and 242−271 (not indicated for reasons of overcrowding) were as dimeric as RNAs 233−271 and 1−271. Symbols have been described in Figure 3. [For comparative purposes the results of Figure 2 are summarized by the thin line-(s). Two thin lines are displayed for RNAs ending downstream of G270: the upper line represents RNAs starting at C233; the lower line represents RNAs starting at G1.]

incubation in high-salt conditions and electrophoresis in TBM/RT. Thus high-salt conditions stimulated the formation of loose dimers by RNAs ending in or near the U5 region. (The U5 region extends from A98 to G181; it is followed by the primer binding site.) Yet, several RNAs ending downstream of G186 (and lacking at least part of the 248−270 region) were monomeric in high-salt conditions. Examples are RNAs 1−234 (Figure 7), 1−401Δ233−251 (Laughrea & Jetté, 1994), and five HIV-1_{Mal} RNAs starting at G1 and mutated only within the 248−270 region (Paillart et al., 1994). The weight of the evidence favors the idea that the dimericity of RNAs 1−66, 1−125, and 1−186 is some truncation artefact, as if nucleotides downstream of G186 normally interacted with nucleotides upstream of G186 (or even A66). It is intriguing that the 62−69 region (GCUUAAGC69) is self-complementary. Perhaps this region is available for dimerization in RNAs 1−125 and 1−186 but unavailable in most longer RNAs. The behavior of RNAs 1−66, 1−125, and 1−186 is reminiscent of the isolated 3′ DLS. The 3′ DLS is a ∼100-nt long region located immediately 3′ of the 5′ splice junction and which spuriously dimerizes in high-salt conditions as indicated by its losing the ability to dimerize when 5′ extended by 28−43 nts (Laughrea & Jetté, 1994). (Longer 5′ extensions result in RNAs that are dimeric simply because they contain an intact 248−270 region.) We conclude that HIV-1 RNAs ending in or near the U5 region contain at least one dimer-promoting sequence, and by analogy with the 3′ DLS, we name this or these sequences "5′ DLS". Consistent with the idea that the 5′ DLS makes no positive contribution to the physiological dimerization process, it is noteworthy that in low-salt conditions, RNAs starting just upstream of the 248−270 region were more dimeric than RNAs starting at or near G1 or C18 (compare lanes 1, 2, and 3 of Figure 2 to lanes 4, 14, and 21 of Figure 2; Laughrea & Jetté, 1994; data not shown), as if the 5′ DLS *inhibited* the dimerization process or at best did not influence it. Among five investigated RNAs ending within the 248−262 region, a variety of dimerization yields was observed in high-salt conditions vs a uniform 0% in low-salt conditions (compare Figure 7 to Figure 2). Two ad hoc ways to reconcile the sizable dimericity of RNAs 233−262 and 1−261 in high-salt conditions with the monomericity of RNA 1−401Δ233−251 is to imagine that the GCGCGC262 and/or the GCU-

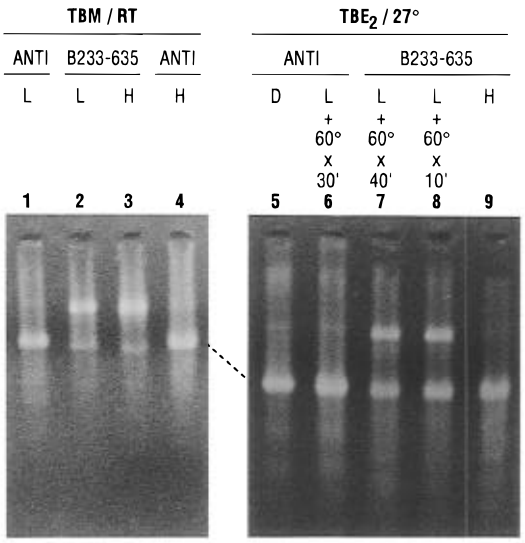

FIGURE 8: Antisense HIV-1 RNA 636−232 does not dimerize. Electrophoretic conditions: 100 V, 1 h (TBM/RT) or as in Figure 6 (TBE_2/27 °C). ANTI, antisense HIV-1 RNA 636−232; B233−635, RNA 233−635; L, H, low- and high-salt conditions, respectively; D, denatured sample.

UAAGC69 autocomplementary sequences are more available for self-hybridization in RNAs 233−262 and 1−261 than in RNA 1−401Δ233−251.

Nevertheless, the two classes of RNAs identified in Figure 2 (which is summarized by the thin line of Figure 7) remain detectable in Figure 7: RNAs ending downstream of G270 were typically 100% dimeric, while all RNAs ending upstream of A263 were at best deficient dimers. We conclude that the 3′ boundary of the dimerization domain is located between A263 and A271 when RNAs are incubated in low-salt conditions and electrophoresed in TBM and that this is still visible in high-salt conditions but less obvious because high ionic strength promotes dimerization of the 5′ DLS in a context-dependent manner. Sequences downstream of the 5′ splice junction, such as the 3′ DLS, had no impact on dimer yield no matter whether the RNAs started at G1, C233, A242, or C248 and no matter whether the study was done at high or low ionic strength. The loose dimers formed in high-salt conditions by several RNAs ending upstream of A263 are called H dimers to indicate that they were unable to dimerize in low-salt conditions or to become tight dimers in buffer L or H.

Antisense HIV-1 RNA Does Not Dimerize. If the integrity of stem C plays a key role in the dimerization process, then an antisense HIV-1 RNA might not be able to dimerize because its U·G base pair (Figure 1a) has become a C×A mismatch. HIV-1 sense RNA 233−635 and antisense RNA 636−232 were compared (Figure 8). Lanes 1−4 show that the antisense could not form loose dimers in either low- or high-salt conditions, contrary to RNA 233−635 which was ≥90% dimeric. Lanes 7−9 show that the antisense could not form tight dimers after 30 min at 60 °C in buffer L, while under the same conditions RNA 233−635 was 60% tight dimer. Other incubations done in buffers L and H and at temperatures ranging from 50 to 70 °C (not shown) indicated that formation of tight dimers by the antisense, if it occurred, was ≥200 times slower than with the sense RNA. The C×A mismatch of the antisense shortens its stem C from 7 to 5 bp and enlarges its loop C by 4 nts. Another structural difference is that the antisense does not have the purine-rich internal loops of the sense RNA (Figure 1a). The simplest explanation for the monomericity of the antisense RNA is that it is handicapped by its combining a 5-bp stem C and a lengthened loop. It is interesting that HIVOYI, an avirulent subtype B virus, has a short 6-bp stem C that includes a terminal U·G base pair (Myers et al., 1990).

DISCUSSION

Relevance of in Vitro Studies. There are now good grounds to believe that the full-length HIV-1 genome can dimerize without nucleocapsid proteins (Fu et al., 1994) and that its thermal stability is at least as high as that of dimeric 5′ end transcripts such as HIV-1 RNAs 1−601 and 1−693 (Fu et al., 1994; Marquet et al., 1994; Paillart et al., 1994). Since no compelling evidence exists in favor of a role for the Pr55gag polyprotein in the dimerization of HIV-1 RNA transcripts (Berkowitz et al., 1993), it is plausible that the HIV-1 genome can dimerize in vivo without the help of proteins. In this and the preceding paper (Laughrea & Jetté, 1994), we have studied 69 HIV-1 RNAs containing different sequences from the 1−790 region of the HIV-1_{Lai} genome. By and large, consistent results were obtained with these RNAs; this self-consistency, coupled to the fact that in all retroviruses studied by electron microscopy, the dimer linkage structure has been localized within the first 600 nts of the genome (Bender & Davidson, 1976; Kung et al., 1976; Bender et al., 1978; Murti et al., 1981), gives confidence that the common folding of these RNAs is not an artefact and that it bears on the in vivo conformation of the dimerization domain of the HIV-1 genome.

Biological Significance of the Kissing-Loop Model of HIV-1 RNA Dimerization. The kissing-loop model of HIV-1 genome dimerization (Laughrea & Jetté, 1994; Skripkin et al., 1994) is appealing because it has at least two physiological connections. (i) It suggests a mechanism for the observation that immature virions have a dimeric HIV-1 genome that is less stable than in mature virions. (ii) The postulated minimal dimerization domain overlaps with an encapsidation signal (see introduction). We had already verified two predictions of the model (Laughrea & Jetté, 1994), namely, (i) the integrity of the 5′ strand of stem C is necessary for dimerization and (ii) RNAs containing little of the 3′ DLS readily dimerize at both low and high ionic strength [see also Marquet et al. (1994) and Muriaux et al. (1995)]. What had not yet been verified was whether (i) the 3′ strand of stem C is necessary for dimerization, (ii) the 248−270 region is sufficient for dimerization, and (iii) whether HIV-1 RNA and the isolated region 248−271 are able to adopt two dimeric forms, one consistent with loop−loop interaction, the other consistent with loop−loop binding plus interstrand bonding of the bases of stem C (Figure 1).

The present paper verifies these three additional predictions of the kissing-loop model of HIV-1 RNA dimerization. (i) The 3′ boundary of the HIV-1 dimerization domain appears located between A263 and A271 (compare lanes 16 and 19 of Figure 2), as if the integrity of stem C was needed for dimerization. (ii) The 248−271 region is necessary and *sufficient* for HIV-1 RNA dimerization (lanes 5, 7, 17, and 19 of Figure 2). (iii) All HIV-1_{Lai} RNAs containing the 248−271 region can form two types of dimers, a loose (low-stability) and a tight (high-stability) dimer (e.g., lanes 3, 8, and 9 of Figure 8).

Two Distinct Conformations. Loose dimers are monomerized by electrophoresis in TBE_2/27 °C as if they involved tertiary structure features (two speculative but plausible examples are shown in Figure 1b,c); tight dimers (or at least tight dimers of HIV-1_{Lai}) are not. We imagine that the tight dimer is a stem C, if not also a stem A and B, that has completely switched from intra- to interstrand bonding (Figure 1d). In the absence of nucleocapsid protein, the loose dimer form might not be a necessary intermediate along the pathway to the tight dimer: at least for RNAs requiring incubation at 60 °C to become tight dimers, the proportion of tight dimers seemed independent of the proportion of loose dimers before heat treatment. It will be interesting to know if nucleocapsid protein catalyzes the formation of tight dimers from preformed loose dimers. It is interesting to note that transcripts of Harvey sarcoma virus RNA can form two types of dimers in vitro, the high-stability dimer requiring a 55 °C heat treatment to appear (Feng et al., 1995).

Constrained Loops Have Higher Self-Affinity. The 248−271 hairpin is analogous to an expanded tRNA anticodon stem−loop. In tRNAs with complementary anticodons, the closure of the two anticodons into hairpin loops increases tRNA−tRNA affinity by a factor 50 (Grosjean et al., 1976). Like the tRNA anticodon stem, stem C might thus function as an affinity enhancer. The control of the copy number of *Escherichia coli* R1 plasmids is linked to the formation of a transient kissing complex formed between the loop of hairpin II of CopA RNA and the complementary loop of hairpin II of antisense CopT RNA. Five to seven nucleotides in the CopA loop result in maximal binding rates in vitro (Hjalt & Wagner, 1992). Perhaps the inability of antisense RNA 636−232 to become a loose dimer is mainly due to its large and less structured hairpin loop and its inability to become a tight dimer is connected to its 5-bp stem C.

Mg^{2+}, Pseudoknots, and HIV-1 RNA Folding. Divalent metal ions are important for RNA folding (Crothers, 1979; Cech, 1993; Yue et al., 1994) and pseudoknot formation in particular (Pleij & Bosch, 1989; Gluick & Draper, 1994). The kissing-loop structure of Figure 1b,c might thus require Mg^{2+} to be stable, contrary to the duplex of Figure 1d whose ionic requirements should be similar to those of a double-stranded helix (Cech, 1993; Jaeger et al., 1990). The presumed need for Mg^{2+} comes from the close juxtaposition of several RNA strands in the loose dimers of Figure 1b,c. Without Mg^{2+}, regions of high negative charge density would be created and formed dimers would be incapable to withstand electrophoresis at elevated ambient temperature in the presence of EDTA. Such juxtaposition of several RNA strands might coordinate a few Mg^{2+} or at least offer a few high-affinity binding sites to Mg^{2+}; this would explain why loose dimers of HIV-1_{Lai} RNAs can withstand electrophoresis at moderate ambient temperatures in the presence of EDTA.[3] The pseudoknot-like structure of Figure 1b is bent in Figure 1c to suggest a possible mechanism for strand-switching between the two stems C (one figuratively grabs the two AA connectors and pulls them down). Pleij et al. (1986) have shown that two nucleotides can easily span a distance of 6 base pairs over the deep groove of double-stranded RNAs. For a double crossing over, the quasi-continuous double helix of Figure 1b might have to bend (Van Belkum et al., 1985; Pleij & Bosch, 1989; Schimmel, 1989). The bending symbolized by Figure 1c may be a natural consequence of the presumption that the two AA connectors cross the same deep groove of the same double-helical section.

The 3′ and 5′ Boundaries of the HIV-1 Dimerization Domain. Together, the present results and previous ones (Laughrea & Jetté, 1994) suggest that the 5′ boundary of the HIV-1 dimerization domain is located at C248 and that the 3′ boundary is located somewhere between A263 and A271, presumably at G270 if, as seems intuitively likely and is suggested by the antisense experiment, what is needed is an intact or near intact stem C. Yet two other domains can dimerize to some extent in the isolated state: the 5′ DLS identified in the present paper and the 3′ DLS (Marquet et al., 1994).

We do not believe that the 5′ DLS plays a physiological role in the dimerization process for the following reasons. (i) The 5′ DLS promotes dimerization under restrictive conditions, such as high-salt conditions (compare Figure 7 and lane 22 of Figure 2 to lanes 10, 12, and 18 of Figure 2). More unspecific RNA−RNA interactions occur at high than at low ionic strength (Bloomfield et al., 1974). Thus RNA interactions that manifest themselves predominantly at high ionic strength might be of questionable biological significance. (ii) When the 5′ DLS is 3′ extended, the resulting more complete and presumably more physiological RNAs, such as RNA 1−234, can lose all ability to dimerize, even at high ionic strength (Figure 7). (iii) The 5′ DLS makes no significant positive contribution to the dimerization kinetics or the dissociation temperature of loose and tight dimers, as shown by the comparative behavior of RNAs starting at G1 or at any of five nucleotides in the range 230−248 (in Figure 2, compare lanes 1, 2, and 3 to lanes 4, 14 and 21; M. Laughrea and L. Jetté, submitted).

The previously proposed downstream dimerization domain (Darlix et al., 1990; Marquet et al., 1991; Sundquist & Heaphy, 1993; Awang & Sen, 1993), i.e., region 295−401, formerly called DLS and now called 3′ DLS, is not necessary for efficient dimerization of HIV-1 RNAs at both low and high ionic strength (lane 2 and 5 of Figure 2; Figure 7). The presence of the 3′ DLS did not increase the stability of HIV-1_{Lai} loose dimers (compare lane 1, top and bottom of Figure 5, to lane 4, top of Figure 5), i.e., did not prevent such RNAs from appearing monomeric after electrophoresis in TBE_2/27 °C. In TBE_2/RT, RNAs having the 248−270 region but lacking the 3′ DLS (or the 5′ DLS) were as dimeric as RNAs containing all these domains (not shown). We believe that the 3′ DLS either plays no role in the dimerization of HIV-1_{Lai} RNAs or plays a role that is completely masked by the presumably strong GCGCGC262 autocomplementary sequence characteristic of HIV-1_{Lai} and all other subtypes B and D HIV-1 viruses[4] (M. Laughrea and L. Jetté, submitted).

[4] All sequenced subtype B and D HIV-1 viruses have a GCGCGC262 autocomplementary sequence. The only apparent exception is HIV-1_{Hxb2}, which reportedly has a CC insertion in the middle of what would otherwise be a GCGCGC sextuplet (Myers et al., 1993). However, strains HIV-1_{Hxbc2}, HIV-1_{Hxb2d}, HIV-$1_{Hxb2gtb}$, and HIV-$1_{Hxb2/Bh10}$ have the HIV-1_{Lai} sextuplet rather than the HIV-1_{Hxb2} octuplet, and we are unaware of anyone actually working with an infectious HIV-1_{Hxb2} strain deprived of an autocomplementary sextuplet. Thus the CC insertion reported in Myers et al. (1993) is either incorrect or misleading. This is easily enough checked: the HIV-1_{Hxb2} sequence of Myers et al. (1993) cannot be cleaved by *Bss*HII; as far as we know, HIV-1_{Hxb2} sequences that are the object of investigations are *Bss*HII cleavable at about nucleotide 260, i.e., where GCGCGC262 is located.

Comparison with Dimers of Genomic RNAs Isolated from HIV-1 Virions. It is interesting that the dissociation temperatures of loose and tight dimers of HIV-1_{Lai} RNAs differ by 15−20 °C (M. Laughrea and L. Jetté, submitted), not unlike the difference between mature and immature dimers of genomic RNAs isolated from HIV-1_{Hxb2} virions (Fu et al., 1994). In addition, loose dimers of HIV-1_{Lai} resist electrophoresis in TBE_2/4 °C but resist less well in TBE_2/RT,[3] in contrast to tight dimers. This parallels the observation that immature genomic RNAs from HIV-1_{Hxb2} virions were never more than half dimeric under electrophoretic conditions comparable to TBE_2/RT, while mature genomic RNAs were almost fully dimeric (Fu et al., 1994). (HIV-1_{Lai} and HIV-1_{Hxb2} are virtually identical viruses; Laughrea & Jetté, 1994; footnote 4.) The simplest explanation for our results and those of Fu et al. (1994) is that immature and mature dimers of genomic RNA contain a 248−270 region respectively in the loose and tight dimeric conformation, without dismissing the possibility that genomic RNA might benefit from additional dimeric interactions within the *gag* gene or perhaps even beyond.

ACKNOWLEDGMENT

We thank Dr. Léa Brakier-Gingras for critical reading of the manuscript, Rhona Rosenzweig and Mary Tomaras for the preparation of the typed text, and Luc Beauchemin and Christine Lalonde for the illustrations.

REFERENCES

Awang, G., & Sen, D. (1993) *Biochemistry 32*, 11453−11457.
Baudin, F., Marquet, R., Isel, C., Darlix, J. L., Ehresmann, B., & Ehresmann, C. (1993) *J. Mol. Biol. 229*, 382−397.
Bender, W., & Davidson, N. (1976) *Cell 7*, 595−607.
Bender, W., Chien, Y. H., Chattopadkyary, S., Vogt, P. K., Gardner, M. B., & Davidson, N. (1978) *J. Virol. 25*, 888−896.
Berkowitz, R. D., Luban, J., & Goff, S. P. (1993) *J. Virol. 67*, 7190−7200.
Bloomfield, V. A., Crothers, D. M., & Tinoco, I., Jr. (1974) *Physical Chemistry of Nucleic Acids*, Harper & Row, New York.
Cech, T. R. (1993) in *The RNA World* (Gesteland, R. F., & Atkins, J. F., Eds) pp 239−269, Cold Spring Harbor Laboratory Press, Cold Spring Harbor, NY.
Crothers, D. M. (1979) in *Transfer RNA: Structure, Properties and Recognition* (Schimmel, P. R., Soll, D., & Abelson, J. N., Eds.) pp 163−176, Cold Spring Harbor Laboratory Press, Cold Spring Harbor, NY.
Darlix, J.-L., Gabus, C., Nugeyre, M.-T., Clavel, F., & Barré-Sinoussi, F. (1990) *J. Mol. Biol. 216*, 689−699.
Feng, Y.-X., Fu, W., Winter, A. J., Levin, J. G., & Rein, A. (1995) *J. Virol. 69*, 2486−2490.
Fu, W., Gorelick, R. J., & Rein, A. (1994) *J. Virol. 68*, 5013−5018.
Gluick, T. C., & Draper, D. E. (1994) *J. Mol. Biol. 241*, 246−262.
Grosjean, H., Soll, D. G., & Crothers, D. M. (1976) *J. Mol. Biol. 103*, 499−519.
Harrison, G. P., & Lever, A. M. L. (1992) *J. Virol. 66*, 4144−4153.
Hjalt, T., & Wagner, E. G. H. (1992) *Nucleic Acids Res. 20*, 6723−6732.
Holbrook, S. R., Cheong, C., Tinoco, I., & Kim, S.-H. (1991) *Nature 353*, 579−581.
Jaeger, J. A., Zuker, M., & Turner, D. H. (1990) *Biochemistry 29*, 10147−10158.
Kim, H.-J., Lee, K., & O'Rear, J. J. (1994) *Virology 198*, 336−340.
Kung, H. J., Hu, S., Bender, W., Bailey, J. M., Davidson, N., Nicolson, M. O., & McAllister, R. M. (1976) *Cell 7*, 609−620.
Laughrea, M., & Jetté, L. (1994) *Biochemistry 33*, 13464−13474.
Laughrea, M., & Moore, P. B. (1977) *J. Mol. Biol. 112*, 399−421.
Levin, J. G., Grimley, P. M., Ramseur, J. M., & Berezesky, I. K. (1974) *J. Virol. 14*, 152−161.
Marquet, R., Baudin, F., Gabus, C., Darlix, J.-L., Mougel, M., Ehresmann, C., & Ehresmann B. (1991) *Nucleic Acids Res. 19*, 2349−2357.
Marquet, R., Paillart, J.-C., Skripkin, E., Ehresmann, C., & Ehresmann, B. (1994) *Nucleic Acids Res. 22*, 145−151.
Méric, C., & Goff, S. P. (1989) *J. Virol. 63*, 1558−1568.
Muriaux, D., Girard, P.-M., Bonnet-Mathonière, B., & Paoletti, J. (1995) *J. Biol. Chem. 270*, 8209−8216.
Murti, K. G., Bondurant, N., & Tereba, A. (1981) *J. Virol. 37*, 411−419.
Myers, G., Rabson, A. B., Berzofsky, J. A., Smith, T. F., Wong-Staal, F., Eds. (1990) *Human Retroviruses and AIDS: A Compilation and Analysis of Nucleic Acid and Amino Acid Sequences*, Los Alamos National Laboratory, Los Alamos, NM.
Myers, G., Korber, B., Wain-Hobson, S., Smith, R. F., & Pavlakis, G. N., Eds. (1993) *Human Retroviruses and AIDS: A Compilation and Analysis of Nucleic Acid and Amino Acid Sequences*, Los Alamos National Laboratory, Los Alamos, NM.
Paillart, J. C., Marquet, R., Skripkin, E., Ehresmann, B., & Ehresmann, C. (1994) *J. Biol. Chem. 269*, 27486−27493.
Peacock, A. C., & Dingman, C. W. (1967) *Biochemistry 6*, 1818−1827.
Pleij, C. W. A., & Bosch, L. (1989) *Methods Enzymol. 180*, 289−303.
Pleij, C. W. A., van Belkum, A., Rietveld, K., & Bosch, L. (1986) in *Structure and Dynamics of RNA* (Van Knippenberg, P. H., & Hilbers, C. W., Eds.) pp 87−98, Plenum Press, New York.
Schimmel, P. (1989) *Cell 58*, 9−12.
Skripkin, E., Paillart, J.-C., Marquet, R., Ehresmann, B., & Ehresmann, C. (1994) *Proc. Natl. Acad. Sci. U.S.A. 91*, 4945−4949.
Sundquist, W. I., & Heaphy, S., (1993) *Proc. Nat. Acad. Sci. U.S.A. 90*, 3393−3397.
Van Belkum, A., Abrahams, J. P., Pleij, C. W. A., & Bosch, L. (1985) *Nucleic Acids Res. 13*, 7673−7686.
Yue, D., Kintanar, A., & Horowitz, J. (1994) *Biochemistry 33*, 8905−8911.

BI951838F